Forward Modeling of Gravity Anomalies for Identification of Burried Cylindrical Body Using Radial Derivative

Muhammad Zuhdi, Syahrial Ayub &Syamsuddin[2]
[1]Physics Education Study Program, University of Mataram, Indonesia
[2]Physics Study Program, University of Mataram, Indonesia
*Corresponding Author: mzuhdi@unram.ac.id

Abstract - Radial Derivative Forward Modeling of Gravity Anomalies for Identification of Cylindrical Geological Features. The gravity method is a geophysical method with exploration costs that are quite cheap compared to other geophysical methods. This method is based on the density contrast of the target body with the surrounding. The cylindrical body is one of the targets among various other geological features. This research was conducted to test the ability of radial derivatives of gravity anomalies for targets in the form of cylindrical body. Radial derivatives consist of a first derivative and a second derivative. Forward modeling of cylindrical geological features is carried out analytically and with finite elements. Both calculations were carried out with a computer program based on Matlab. The results show that there is no difference in results either analytically or finite element wise. This method has been proven to be able to provide clear boundary positions on cylindrical geological features.

INTRODUCTION

The gravity method is a reliable exploration method and is very cheap compared to the seismic method. Gravity data is also used as a binding data from seismic methods. Gravitational methods are also used in mineral exploration to clarify information that has been obtained from electromagnetic methods. Gravity methods are also sometimes used for engineering and archaeological purposes (Telford et al., 1990). The gravity method is a geophysical method that was first used for petroleum exploration (Nabighian et al, 2005). Gravity interpretation is an attempt to obtain mass distribution from gravity data on the surface. The interpretation of gravity is actually an inversion process from field theory, because the known value is the potential while the source is something that will be sought (Agung and Barat 1965).

The 4D microgravity method or also known as time lapse microgravity is a development of the gravity method with the fourth dimension, namely time. This method is also characterized by repeated daily, weekly, monthly or yearly measurements using very high accuracy gravity measurements supported by high accuracy position and altitude measurements. The advantage of this method is that its operation is relatively simple and environmentally friendly (Reynold, 1997).

The 4D gravity method has been widely used for identifying and monitoring subsurface changes. Eiken et al., used inter-regional microgravity to monitor gas production in underwater reservoirs with a gravimeter sensitivity of up to 4 micro Gal. The level of confidence in the measurement results is 80% (Eiken, et al. 2004). Gettings et al. (2002), measured 4D microgravity values around geothermal geyser sources to detect subsidence due to mass changes during the production period with an anomaly rate of 2 ± 2 microGal and 4D of 10 ± 8 microGal (Gettings et al., 2002) Akasaka and Nakanishi (2000) separating geothermal source gravity anomalies from the influence of groundwater changes by correlating

drilling data and rainfall data (a=Akasaka and Nakanishi Rahman et al. (2007) succeeded in monitoring fluid injection in reservoirs in South Sumatra using the 4D gravity method (Rahman et al, 2007). Davis et al. (2008), measured 4D gravity anomalies to monitor water injection rates in the artificial aquifer storage and recovery (ASR) aquifer in Leyden Colorado. 2008). Sarkowi (2008) examined the relationship between changes in ground water and changes in vertical gravity gradient values in the city of Semarang and its surroundings. Zuhdi and Sismanto (2013) have created a horizontal model of geological features and their derivative treatment. Ricardi et al, (2022) created a tidal gravity model for the first time. Sprlak et al. (2018) created a density distribution map on the moon using gravity data. Tanzer et al., created a model of the earth's crust using the gravity method with harmonic analysis. Kumar et al, (2023) utilized the gravity method with a superconductor gravimeter to examine aquifer boundaries. Kuhn and Hirt (2016) use the second derivative of gravity data to find topography.

In this research, the radial derivative gravity method will be used to detect geological features with a cylindrical shape. Cylindrical geological features are often found in various places around the world. These geological features include magmatic intrusions on volcanoes, volcanic plateaus or what are called plateaus, melted magma on molten volcanoes and intrusions of various plutonic rocks. Forward modeling is carried out in two ways, namely analytical and finite element modeling using a Matlab-based program whose algorithm was designed by the author himself.

RESEARCH METHODS

Radial Derivative is the derivative of the gravitational anomaly value against the horizontal distance in the radial direction from a certain point which is considered the center of the anomaly. The horizontal derivative of a gravity anomaly is the derivative of the gravity value in a certain straight line direction. If the straight line cuts perpendicularly to a density contrast boundary, the derivative value will be large. In many cases it is necessary to obtain a derivative that is always perpendicular or as close to perpendicular as possible to the anomalous density contrast. For this purpose, Radial Derivatives were created. The center point of the Radial Derivative is selected based on certain considerations so that this point is considered or considered as the center of the anomaly to be identified.

The value of the gravity anomaly $\Delta gz(x,y,z)$ caused by the density anomaly $\Delta\rho(\alpha,\beta,\gamma)$ is written as:

$$\Delta g_z(R,z,\lambda)$$
$$= -G \int_0^\infty \int_{-\infty}^\infty \int_{-\infty}^\infty \frac{\Delta\rho\,(R',z',\lambda')(z-z')}{\{(Rcos\lambda - Rcos\lambda')^2 + (Rsin\lambda - Rsin\lambda')^2 + (z-\gamma)^2\}^{3/2}}\,RdR\,dz'\,d\lambda'$$

(1)

can be converted into cylindrical coordinates, so that $\Delta gz(x,y,z)$ becomes $\Delta gz(R,z,\lambda)$ and $\Delta\rho(R',z',\lambda')$, with the relationship: $x = R \cos \lambda$, $y = R \sin \lambda$ and $z =$ z, while $\alpha = R \cos \lambda'$, $\beta = R \sin \lambda'$ and $\gamma = z'$, with the mass element $\Delta\rho\,dR\,dz\,Rd\lambda$ so that the gravity value towards the z axis can be written as:

$$\Delta g_z(x,y,z) = -G \int_0^\infty \int_{-\infty}^\infty \int_{-\infty}^\infty \frac{\Delta\rho\,(\alpha,\beta,\gamma)(z-\gamma)}{\{(x-\alpha)^2 + (y-\beta)^2 + (z-\gamma)^2\}^{3/2}}\,d\alpha\,d\beta\,d\gamma$$

(2)

The First Derivative Radial (FDR) of the gravity anomaly at vertical cylindrical

coordinates Δgz(R,z,λ) can simply be written as:

$$FRD = \frac{\partial \Delta g_z(R,z,\lambda)}{\partial R}$$

$$FRD = \frac{\partial}{\partial R}\left[\int_0^\infty \int_{-\infty}^\infty \int_{-\infty}^\infty \frac{\Delta\rho\,(R',z',\lambda')(z-z')}{\{(x-\alpha)^2+(y-\beta)^2+(z-\gamma)^2\}^{\frac{3}{2}}} R\,dR\,dz\,d\lambda\right]$$

(3)

Meanwhile, the second Radial Derivative (SRD) can simply be written as:

$$SRD = \frac{\partial^2 \Delta g_z(R,z,\lambda)}{\partial R^2}$$

$$SRD = \frac{\partial^2}{\partial R^2}\left[\int_0^\infty \int_{-\infty}^\infty \int_{-\infty}^\infty \frac{\Delta\rho\,(R',z',\lambda')(z-z')}{\{(x-\alpha)^2+(y-\beta)^2+(z-\gamma)^2\}^{\frac{3}{2}}} R\,dR\,dz\,d\lambda\right]$$

(4)

Equation (4) is an FRD and SRD equation that can be described analytically if the model geometry of the source is known and has a simple form. This analytical formulation is useful for knowing the graphical behavior of the gravity anomaly. This analytical equation is also needed in creating a Radial Inversion model from the model.

Radial Derivatives can be viewed as directional derivatives with a radial direction that is always away from a certain central point as the center of the Radial Derivative. If the gravitational field g is considered as a scalar field on a flat plane (x,y), then the largest rate of change in the value of g(x,y) on that plane is the gradient of the g field which is written as:

$$\nabla\,g_{(x,y)} = \left(\frac{\partial g_{(x,y)}}{\partial x}\hat{\imath} + \frac{\partial g_{(x,y)}}{\partial y}\hat{\jmath}\right)$$

(5)

If the radial direction in the Radial Derivative is vector v which is the unit direction vector, then the Radial Derivative of the field g(x,y) can be written as:

$$DRg(x,y) = \nabla\,g_{(x,y)} \cdot v$$

(6)

At the coordinate position (a, b), the field gradient g(x,y) becomes ∇ g(a,b) and the direction of the Radial Derivative becomes:

$$DRg(a,b) = \nabla\,g_{(a,b)} \cdot v$$

(7)

The direction of v is always away from the center of the Radial Derivative so that at position (a, b), the unit vector in the direction of v can be written as:

$$v = \frac{a\hat{\imath}+b\hat{\jmath}}{\left|\sqrt{a^2+b^2}\right|}$$

Thus the Radial Derivative of the g field at point (a, b) can be written as:

$$DRg(a,b) = \nabla\,g_{(a,b)} \cdot \frac{a\hat{\imath}+b\hat{\jmath}}{\left|\sqrt{a^2+b^2}\right|}$$

(8)

Figure 1 shows the field gradient g which is a directional derivative towards the unit vector position v. The value of the change in the gravitational field in the Radial Derivative is always smaller than the g field gradient in the (x, y) plane and can have a maximum value equal to the g field gradient.
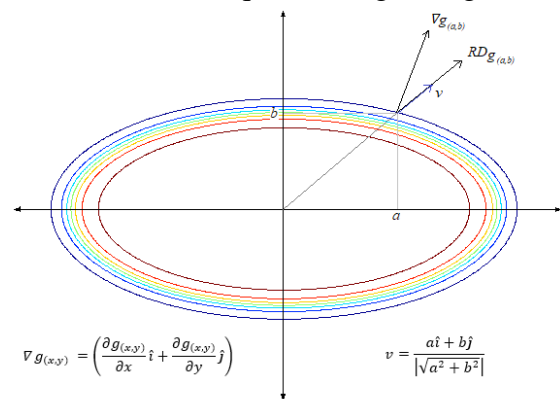

Figure 1. Field gradient g and directional derivative towards v

Radial derivatives can be approached discretely by subtracting each measurement point in a certain direction. The derivative towards the x axis is obtained by subtracting the gravity value from the measurement at

point x_{n+1}, namely g_{n+1}, from the gravity value at point x_n, namely g_n, then dividing by the distance x_{n+1} to x_n. To get the derivative value towards the y axis, it is obtained by subtracting the gravity value from the measurement at point y_{n+1} from the gravity value at point y_n and then dividing it in the same way by the distance y_{n+1} to y_n. The value of the derivative approach in the direction of the y-axis is $(g_{n+1}-g_n)/(y_{n+1}-y_n)$ shown by the red slope in Figure 3. (a). In the same way, the value of the derivative approach towards the y-axis is $(g_{m+1}-g_m)/(y_{m+1}-y_m)$.
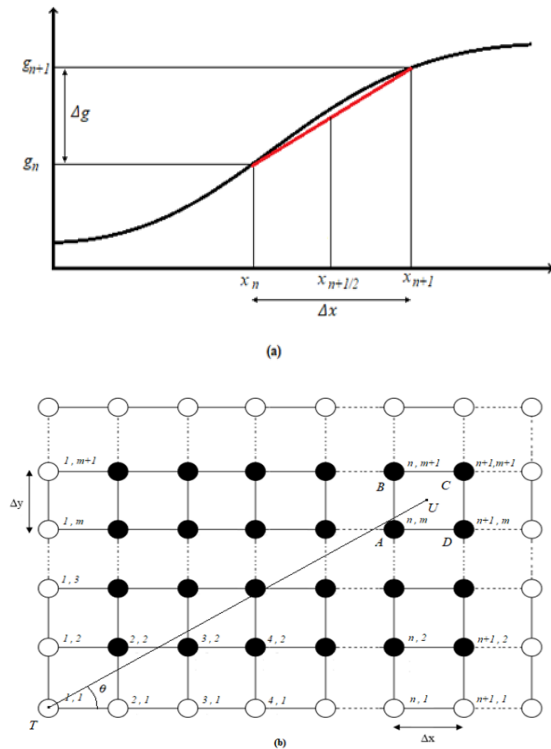

Figure 2. (a) Horizontal derivative approach (b) Dotted diagram showing positions for Radial Derivative calculations

In many cases, a derivative is needed not only in the direction of the x or y axis but in a certain direction, which is often called a directional derivative.

In Figure 2, Δx is the approximation of the horizontal derivative value towards the x axis at position n+1/2,m, so that Δx in this equation can be written as:

$$\frac{\Delta gx_{n+1/2,m}}{\Delta x} = \frac{g_{n+1,m}-g_{n,m}}{x_{n+1,m}-x_{n,m}} \qquad (9)$$

in the same way, then dy which is the horizontal derivative towards the y axis at position n+1/2, m can be written as:

$$\frac{\Delta gy_{n,m+1/2}}{\Delta y} = \frac{g_{n,m+1}-g_{n,m}}{y_{n,m+1}-y_{n,m}} \qquad (10)$$

By looking at Figure 2. (b), the values of cos θ and sin θ have values whose magnitude can be expressed as:

$$\cos \theta = \frac{x_{n+1/2,1}-x_{1,1}}{\left\{(x_{n+1/2,1}-x_{1,1})^2+(y_{1,m+1/2}-y_{1,1})^2\right\}^{1/2}}$$

$$\sin \theta = \frac{y_{1,m+1/2}-x_{1,1}}{\left\{(x_{n+1/2,1}-x_{1,1})^2+(y_{1,m+1/2}-y_{1,1})^2\right\}^{1/2}}$$

$$(11)$$

The Radial Derivative Value $\Delta g/\Delta R=(\Delta gx/\Delta x)\sin \theta+(\Delta gy/\Delta y)\sin \theta$ is then obtained by substituting it with equations (9), (10), and (11) which can be written as:

$$\frac{\Delta g}{\Delta R} = \frac{g_{n+1,m}-g_{n,m}}{x_{n+1,m}-x_{n,m}} \frac{x_{n+1/2,1}-x_{1,1}}{\left\{(x_{n+1/2,1}-x_{1,1})^2+(y_{1,m+1/2}-y_{1,1})^2\right\}^{1/2}}$$
$$+ \frac{g_{n,m+1}-g_{n,m}}{y_{n,m+1}-y_{n,m}} \frac{y_{1,m+1/2}-x_{1,1}}{\left\{(x_{n+1/2,1}-x_{1,1})^2+(y_{1,m+1/2}-y_{1,1})^2\right\}^{1/2}}$$

$$(12)$$

The Radial Derivative Program can be seen in Appendix 1. This program can be used for data with a regular grid called matrix X, with an odd number of columns and rows.

RESULTS AND DISCUSSION
Results

Cylindrical geological features are often found in various places around the world. These geological features include magmatic intrusions on volcanoes, volcanic plateaus or what are called plateaus, melted magma on molten volcanoes and intrusions of various plutonic rocks. The main requirement for detecting cylindrical geological features is the density contrast of the cylindrical rock with respect to the surrounding rocks.

The gravity anomaly at the measurement point on the surface as shown in Figure 3 was formulated by Telford et al. (1990) with equation (13). This equation applies to cylinders of infinite length, or whose length is very much greater than the depth of the top of the cylinder. In the case of a cylindrical geological feature, it can be calculated by subtracting two infinitely long cylinders of different depths.

Figure 3. shows the thin cylinder approach with a reduction of 2 infinite long cylinders. From this image it can be seen that the thickness of the geological feature is $z_2 - z_1$ with the peak depth of the geological feature being z_1.

For a cylinder whose length is much greater than the depth at its top, if it satisfies the Laplace equation, it can be expressed $r > z > R$ in the form of a Legendre polynomial with the formulation:

$$g(r,\theta) = k \sum_{n=0}^{\infty} b_n r^{-(n+1)} P_n (\cos \theta) \quad (13)$$

with the value k = 12.77.10-3 ρ, b_n is the coefficient, P_n (cos θ) is the Legendre polynomial, $r^2 = x^2 + z^2$, and θ = arc tan (x/z). On the cylinder axis r = z so that $\theta = 0$, then the equation becomes

$$g = k(\frac{b_0 P_0}{z} + \frac{b_1 P_1}{z^2} + \frac{b_2 P_2}{z^3} + \frac{b_3 P_3}{z^4} + \cdots)$$

$$g = k(\frac{b_0}{z} + \frac{b_1}{z^2} + \frac{b_2}{z^3} + \frac{b_3}{z^4} + \cdots) \quad (14)$$

with P_0, P_1, P_2 and so on are Legendre polynomials with value 1.

For values of L approaching infinity, we obtain the equation

$$g = 12{,}77 \times 10^{-3} \rho (\sqrt{x^2 + z^2} - z) \quad (15)$$

The expansion of equation (15) in the form (R/z) is obtained

$$g = k(\frac{R^2}{2z} - \frac{R^4}{8z^3} + \frac{R^6}{16z^5} - \frac{5R^8}{128z^7} + \cdots) \quad (16)$$

The value $b_n = 0$ applies to odd n, while $b_0 = R^2/2$, $b_2 = -R^4/8$, $b_4 = R^6/16$, $b_6 = 5R^8/128$ and so on. So g(r, θ) outside the cylinder axis becomes

$$g(r,\theta) = 12{,}77 \times 10^{-3} \rho R \left\{ \frac{1}{2}\left(\frac{R}{r}\right) - \frac{1}{8}\left(\frac{R}{r}\right)^3 P_2(\mu) + \frac{1}{16}\left(\frac{R}{r}\right)^6 P_4(\mu) - \frac{5}{128}\left(\frac{R}{r}\right)^7 P_6(\mu) + \cdots \right\} \quad (17)$$
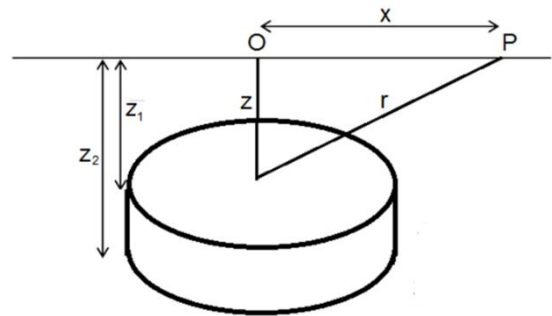
with the value μ = cos θ.

Figure 3. Approach to a thin cylinder with a difference between 2 long cylinders and infinite downwards

For a small cylinder or vertical rod with cross-sectional area A, depth z and length L, it can be formulated as

$$g = 2{,}03 \times 10^{-3} A\rho \left[\frac{1}{(x^2+z^2)^{0.5}} - \frac{1}{\{(z+L)^2+x^2\}^{0.5}}\right] \quad (18)$$

by substituting $r = (x^2+z^2)^{1/2}$, we get

$$g(r,\theta) = 6.4 \times 10^{-3} \rho R^2 \left\{ \frac{1}{(x^2+z^2)^{0.5}} - \frac{R^2 P_2(\mu)}{4(x^2+z^2)^{1.5}} + \frac{R^4 P_4(\mu)}{16(x^2+z^2)^{2.5}} - \cdots \right\}$$

$$(19)$$

The equation has better accuracy than equation (18). This equation was chosen because it is simpler.

For values z < R, another approach to equation (19) is not in the form R/z but in the form z/R, we get:

$$g = 12.77 \times 10^{-3} \rho R^2 \left(1 - \frac{z}{R} + \frac{z^2}{2R^2} - \frac{z^4}{8R^4} + \frac{z^6}{16R^6}\right) \quad (20)$$

for z < r < R, the off-axis value equation can be expressed in the form

$$g(r,\theta) = k \sum_{m=0}^{\infty} a_m r^m P_m(\mu)$$

$$= k \{a_0 + a_1 r\, P_1(\mu) + a_2 r^2 P_2(\mu) + a_3 r^3 P_3(\mu) + \cdots\} \quad (21)$$

So the coefficient on the axis (r = z, θ = 0) is obtained

a_0 = R, a_1 = -1, a_2 = 1/2R, a_3 = a_5 = a_{2n+1} = 0, a_4 =1/8 R^3, …

So, for outside the z axis, the equation for z ≤ r ≤ R, becomes

$$g(r,\theta) = 2\pi G\rho R \left\{1 - \left(\frac{r}{R}\right)P_1(\mu) + \frac{1}{2}\left(\frac{r}{R}\right)^2 P_2(\mu) - \frac{1}{8}\left(\frac{r}{R}\right)^4 P_4(\mu) + \cdots\right\} \quad (22)$$

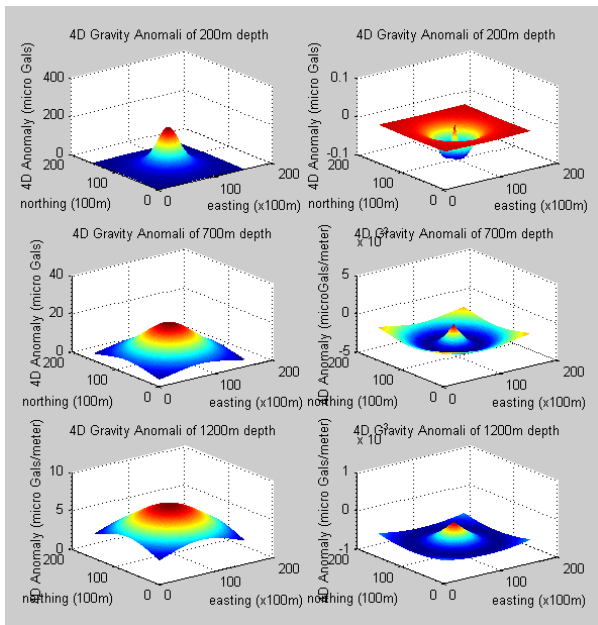In Figure 3. it appears that the radial direction is the x direction.

Figure 4. Gravity anomalies of cylindrical geological features and Radial Derivatives for various depths calculated analytically

By replacing r in each term of equation (22) with x2 + z2 and deriving each term we get:

$$\frac{\partial g}{\partial x}(x,\theta) = 2\pi G\rho R \left\{1 - \left(\frac{1}{R\sqrt{x^2+z^2}} - \frac{x^2}{R(x^2+z^2)^{3/2}}\right)P_1(\mu) + \frac{1}{2}\left(\frac{2x}{R^2}\right)P_2(\mu) \frac{1}{2}\left(\frac{x^2+z^2}{R^4}\right)P_4(\mu) + \cdots\right\} \quad (23)$$

For R values between r and z, with r < R < z, we use a different series, namely with the equation:

$$g(r,\theta) = 2\pi G\rho R \left\{\frac{1}{2}\left(\frac{R}{r}\right) + \frac{1}{8}\left(\frac{R}{r}\right)^3 P_2(\mu) - \frac{1}{16}\left(\frac{R}{4}\right)^5 P_4(\mu) + \cdots\right\} \quad (24)$$

As with replacing *r* in each term of equation (22), *r* in equation (24) is also replaced with $x^2 + z^2$ and the Radial Derivative is obtained by deriving each term so that we get:

$$g(r,\theta) = 2\pi G\rho R \left\{\frac{1}{2}\left(\frac{-Rx}{(x^2+z^2)^{3/2}}\right) + \frac{3}{8}\left(\frac{-R^3 x}{(x^2+z^2)^{5/2}}\right)P_2(\mu) - \frac{15}{16}\left(\frac{R^5 x}{(x^2+y^2)^{3/2}}\right)P_4(\mu) + \cdots\right\} \quad (25)$$

Figure 4 shows the geological feature anomalies with various depths as well as the Radial Derivatives for various corresponding depths calculated analytically.

Discussion

First Radial Derivative (FRD) is the first horizontal derivative in a radial direction concentric to a certain point which is considered to represent the center of the

anomaly. Visually, FRD can show the density contrast limits quite well. Performing FRD on gravity anomalies can provide a lot of additional information about the density contrast limits in the area.

Second Radial Derivative (SRD) is a second horizontal derivative in a radial direction concentric to a certain point which is considered to represent the center of the anomaly or center of mass being explored. Visually, FRD can show the density contrast boundaries very sharply. To increase the sharpness of the anomaly, cutting can be done on the SRD value. With cutting treatment, the SRD of the anomaly will visually show very sharp boundaries of the density contrast. Performing FRD on gravity anomalies can provide a lot of additional information about density contrast limits through visual display. This SRD method will enrich the instrument for interpreting gravity anomalies, especially vertical density contrast anomalies.

CONCLUSION

This modeling can be applied to geological features that have a cylindrical shape or that resemble a cylinder such as ellipses and cylinders with conical roofs. Finite difference modeling based on convolution should be carried out to continue research on this cylindrical geological feature.

REFERENCES

Akasaka, C., & Nakanishi, S. (2000). Evaluation of Microgravity Background at the Undisturbed Oguni Geothermal Field, Japan. *Proceedings, Twenty-Fifth Workshop on Geothermal Reservoir Engineering Stanford University*.

Davis, K., Li, Y., & Batzle, M. (2008). Time-lapse gravity monitoring: A systematic 4D approach with application to aquifer storage and recovery. *Geophysics*, *73*(6), WA61-WA69.

Eiken, O., Stenvold, T., Zumberge, M., Alnes, H., & Sasagawa, G. (2008). Gravimetric monitoring of gas production from the Troll field. *Geophysics*, *73*(6), WA149-WA154.

Grand, F.S. & West, G.F. (1965). *Interpretation Theory injeksi Applied Geophysics*, McGraw Hill Inc..

Gettings, P., Harris, R. N., Allis, R. G., & Chapman, D. S. (2002). Gravity signals at the Geysers geothermal system. *Transactions-Geothermal Resources Council*, 425-430.

Kumar, S., Rosat, S., Hinderer, J., Mouyen, M., Boy, J. P., & Israil, M. (2023). Delineation of aquifer boundary by two vertical superconducting gravimeters in a karst hydrosystem, France. *Pure and Applied Geophysics*, *180*(2), 611-628. https://doi.org/10.1007/s00024-022-03186-7

Kuhn, M., & Hirt, C. (2016). Topographic gravitational potential up to second-order derivatives: an examination of approximation errors caused by rock-equivalent topography (RET). *Journal of Geodesy*, *90*(9), 883-902. DOI 10.1007/s00190-016-0917-6

Nabighian, M.N., Ander,M.E., Grauch, V.J.S.,Hansen, R.O., LaFehr, T.R., Li, Y., Pearson, W.C., Pierce, J.W., Phillips, J.D., and Ruder, M.E. (2005). 75th Anniversary: Historical development of the gravity method in exploration, *Geophysics*, Vol. 70 (6),. P 63ND-89ND.

Rahman, A., Mashud, M. I., Rahmawati, A. D., Susilo, A., & Sarkowi, M. (2007). Hydrocarbon Reservoir Monitoring Using Gravity 4d Method, In "X" Field in Southern Sumatra Area. In *Proceedings Joint Convention Bali 2007The 32nd HAGI And The 36th IAGI Annual Convention and Exhibition*.

Reynolds, J.M. (1997). *An introduction to applied and environmental geophysics.* John Wiley & Sons, Chichester

Riccardi, U., Hinderer, J., Zahran, K., Issawy, E., Rosat, S., Littel, F., & Ali, S. (2023). A first reliable gravity tidal model for lake Nasser region (Egypt). *Pure and Applied Geophysics*, *180*(2), 661-682. https://doi.org/10.1007/s00024-022-03087-9.

Sarkowi, M., Kadir, W.G.A., Santoso. Dj. (2005). Strategy of 4D Microgravity Survey for the Monitoring of Fluid Dynamics in the Subsurface, *Proceedings World Geothermal Congress*, Antalya, Turkey, 24-29 April 2005

Šprlák, M., Han, S. C., & Featherstone, W. E. (2018). Forward modelling of global gravity fields with 3D density structures and an application to the high-resolution (~ 2 km) gravity fields of the Moon. *Journal of Geodesy*, *92*(8), 847-862. https://doi.org/10.1007/s00190-017-1098-7

Telford, W.M., Geldart, L.P., Sherif, R.E., and Keys, D.A. (1990). *Applied Geophysics*. Cambridge University Press: Cambridge.

Tenzer, R., Novák, P., Vajda, P., Gladkikh, V., & Hamayun. (2012). Spectral harmonic analysis and synthesis of Earth's crust gravity field. *Computational Geosciences*, *16*, 193-207. DOI 10.1007/s10596-011-9264-0

Zuhdi, M., & Sismanto. (2013). Response Of Time Lapse Gravity Anomaly Model Of Gas Injection In Reservoir And Water Table Changes On It's Near Surface. *Proceedings of Basic Sciences Converence* 2013, Brawijaya University.